Int. J. Solids Structures Vol. 17, No. 10, pp. 995–1004, 1981
Printed in Great Britain.

0020-7683/81/100995-10$02.00/0

FLEXURE STRENGTH AND FRACTURE OF POLYMETHYLMETHACRYLATE PLATES

Y. M. TSAI and Y. T. CHEN

Engineering Science and Mechanics, Iowa State University, Ames, IA 50011, U.S.A.

(*Received* 30 *September* 1980; *in revised form* 30 *January* 1981)

Abstract—The flexure strength of a polymethylmethacrylate (PMMA) plate is investigated. The plate resting on a ring foundation is subjected to either a quasi-static contact load or the impact load of a spherical projectile. The dynamic fracture load required to fracture the plate specimen is measured to be about 30% higher than the quasi-static fracture load. The piezoelectric accelerometer used to measure the impact load clearly detects the occurrence of fracture as a sudden drop in its signal output. General formulas for the contact between the spherical indenter and the thin plate specimen are obtained to determine the normal contact stress and the critical tensile stress in the plate.

The speed of a crack propagating in a PMMA plate specimen under transverse loadings is measured experimentally. Since small in-plane stretching stress is produced in the specimen in the experimental arrangement, the crack speeds measured are small, compared to the limiting crack speed of the material.

INTRODUCTION

The problem of contact between a spherical body and a plate or panel was involved in the instrumented projectile impact test developed in [1] and in the studies of foreign object impact damage to composite plates or panels[2, 3]. Localized damages in the form of branching *Y*-shaped cracks were observed in plate specimens subjected to the impact of spherical projectiles[1, 3]. The internal stresses in an anisotropic plate were determined using a finite-element computer program[3].

The critical point in the plate specimens used in [1, 3] is at the surface point opposite the center of the contact area between the spherical projectile and the plate. If the force developed between the projectile and the plate is idealized as a concentrated load, the stress at the critical point becomes infinitely large in the classical theory of the plate[4, 5]. To determine the critical stress in the thin plate, the force should be treated as a contact force which is distributed in a certain manner over the contact area between the spherical body and the thin plate specimen[4–6].

The problem of contact for a finitely thick plate which is subjected to the identation of a spherical body on a surface and supported by a circular ring foundation on the other surface was solved in terms of the three-dimensional equations of equilibrium[7]. The normal contact stress was solved from an integral equation through the process of successive approximation, using an electronic computer. The stress components were written in terms of non-dimensional functions, which were also calculated using an electronic computer[7]. In the present problem the three-dimensional solutions presented in [7] are linearized for small value of plate thickness. General equations are obtained to determine the critical stress in a thin plate which is subjected to the contact force of a spherical body.

Two sets of experiments on the flexure fracture of polymethylmethacrylate (PMMA) plates are also carried out in the present work. The first set is concerned with the measurement on the flexure strength of a PMMA plate. The specimen is made of a PMMA plate of 1/16″ thickness, which is loaded under the same conditions as defined in the above theory until fracture occurs. The load was produced by a Material Test System (MTS) machine or the impact of a steel ball. A piezoelectric accelerometer was used to measure the acceleration of the steel ball in the impact test. The loads required to fracture the specimens were measured, and the flexure strength of the PMMA plate under quasi-static and impact loadings was determined. The patterns of flexure fracture were also observed. In the second set of experiments, the speed of the flexure crack propagating in a 1/8″ thick PMMA plate was measured. The loading arrangements and the techniques of crack-speed measurements are similar to those described in an earlier work on the flexure fracture in glass plates[8].

STRESS ANALYSIS

In the three-dimensional plate contact problem [7], cylindrical coordinates (r, θ, z) were used, z being normal to the plate surface. A spherical indenter of radius R was pressed on the upper plate surface $z = H$, whereas the lower plate surface $z = -H$ was axisymmetrically supported on a ring foundation of radius ρ. The normal contact stress in the contact area was denoted as $p(r)$ which is equal to zero for $r > a$, a being the radius of the contact area. The shape of the indenter in the contact area was written as $g(r)$. The solution was written as the sum of the symmetrical (stretching) and the antisymmetrical (bending) components [7]. For the present calculations, the same notations are retained. For small value of H, the symmetrical component of the vertical displacement at $z = H$ in eqn (14) in [7] is small and neglected, compared to the antisymmetrical (bending) component. For small H eqns (13) and (15) in [7] for the indenter-shape function can now be written in terms of the zeroth order Bessel function J_0 for $r \le a$ as follows:

$$g(r) = C\int_0^\infty \bar{p}_{II}(s)[1 + Q_{II}(s)]J_0(rs)\,ds - U_z(0,0) \tag{1}$$

where

$$\bar{p}_{II} = \frac{1}{2}\left[\int_0^a p(r)rJ_0(sr)\,dr - PJ_0(\rho s)/2\pi\right] \tag{2}$$

and the total normal contact force is denoted by

$$p = 2\pi\int_0^a p(r)r\,dr. \tag{3}$$

The constant $C = (1-\nu)/\mu$ involves Poisson's ratio ν and the shear modulus μ. The functions Q_{II} and $U_z(0,0)$ are respectively defined in eqns (18) and (12) in [7].

The process to convert eqn (1) into an integtal equation for determining the unknown $p(r)$ is the same as that used in [7]. However, the integration of the first term in the bracket in eqn (1), associated with the second term on the right hand side of eqn (2), requires new calculations using the identities in [9] for $r \le a$ as follows:

$$\frac{\partial}{\partial r}\int_r^a \frac{\zeta\,d\zeta}{\sqrt{\zeta^2 - r^2}}\frac{\partial}{\partial\zeta}\int_0^\zeta \frac{m\,dm}{\sqrt{\zeta^2 - m^2}}\left[\int_0^\infty J_0(\rho s)J_0(ms)\,ds\right]$$
$$= rA_1(r,\rho) - r[(a^2 - r^2)(\rho^2 - a^2)]^{-1/2} \tag{4}$$

where

$$A_1 = \int_r^a [(\zeta^2 - r^2)(\rho^2 - \zeta^2)^3]^{-1/2}\zeta\,d\zeta. \tag{5}$$

If the above operations over the quantities in the bracket are applied over eqn (1), the results after integrations by parts lead to two equations [7] as follows:

$$p(r) = p_0 - \frac{2}{\pi}A_1B_1 - \frac{4}{\pi}F \tag{6}$$

and

$$g(0) + \int_0^a \frac{ag'(m)\,dm}{(a^2 - m^2)^{1/2}} = -\frac{C}{2}\int_0^a \frac{p(\lambda)\lambda\,d\lambda}{(\rho^2 - a^2)^{1/2}} +$$
$$C\int_0^\infty \bar{p}_{II}Q_{II}\cos(sa)\,ds - U_z(0,0) \tag{7}$$

where

$$F = \int_0^\infty \int_r^a \frac{\sin(s\zeta)\bar{p}_{II}Q_{II}s \, d\zeta \, ds}{(\zeta^2 - r^2)^{1/2}} \tag{8}$$

$$B_1 = \int_0^a p(\lambda)\lambda \, d\lambda \tag{9}$$

and

$$p_0 = -\frac{4}{C\pi}\int_r^a \frac{d\zeta}{(\zeta^2 - r^2)^{1/2}} \frac{\partial}{\partial \zeta}\int_0^\zeta \frac{\zeta g'(m)\, dm}{(\zeta^2 - m^2)^{1/2}}. \tag{10}$$

The primes in eqns (6) and (7) denote partial differentiations. For a spherical indenter, the indenter-shape function can be written as:

$$g = r^2/2R - \alpha \tag{11}$$

where R is the indenter radius, and α is the distance of approach between the indenter and the plate[7]. In terms of (11), eqn (10) is integrated as

$$p_0 = -\frac{8}{C\pi R}(a^2 - r^2)^{1/2}. \tag{12}$$

In order to integrate the integral in (8), eqn (2) can be written in terms of (3) as

$$\bar{p}_{II} = \frac{1}{2}\int_0^a \int_\lambda^\rho J_1(sm)s \, dm \, p(\lambda)\lambda \, d\lambda. \tag{13}$$

For small value of H, Q_{II} in [7] can be approximated by $3/(2H^3s^3)$. Furthermore, the contact radius a is small compared to ρ[7]. The integration over ζ in (8) is integrated by parts as follows:

$$\int_r^a \frac{\sin(s\zeta)\, d\zeta}{(\zeta^2 - m^2)^{1/2}} = \frac{(a^2 - r^2)^{1/2}}{a}\sin(sa) - \int_r^a \sqrt{\zeta^2 - r^2}\, \frac{\zeta\cos(s\zeta)s - \sin(s\zeta)}{\zeta^2}\, d\zeta. \tag{14}$$

If the transformations $s = u/\rho$ and $\zeta = a\eta$ are introduced, the last term on the r.h.s. of eqn (14) can be seen to be of the order of $(a/\rho)^3$ and is then dropped, compared to the preceding term. The integral in (8) can now be integrated in terms of eqns (13) and (14) as follows[9]:

$$F = (a^2 - r^2)^{1/2}B_2 \tag{15}$$

where

$$B_2 = \frac{3}{4H^3}\int_0^a p(\lambda)\lambda\left[-\ln\frac{a}{\rho} + \frac{(a^2 - \lambda^2)}{a} - \ln\left(1 + \frac{\sqrt{a^2 - \lambda^2}}{a}\right)\right] d\lambda. \tag{16}$$

In terms of (5), (9), (12) and (16), the integral eqn (6) can be seen as a Fredholm equation with degenerate kernels[10]. The solution of eqn (6) is obtained[10] and describes the distribution of the normal contact stress $p(r)$ in terms of the results as follows:

$$B_1 = -8a^3/(3C\pi R\Delta) \tag{17}$$

$$B_2 = B_1\frac{9}{4H^3}\left[\epsilon_1 + \frac{2}{\pi}\left(\epsilon_1 - \frac{1}{3}\ln\frac{\rho}{a}\right)\epsilon_2\right] \tag{18}$$

where

$$\Delta = 1 + \frac{3a^3}{\pi H^3}\epsilon_1 + \frac{2}{\pi}\left(1 + \frac{3a^3}{\pi H^3}\epsilon_1 - \frac{a^3}{\pi H^3}\ln\frac{\rho}{a}\right)\epsilon_2 \tag{19}$$

$$\epsilon_1 = \frac{1}{3}\ln\frac{\rho}{a} + \frac{1}{4} - \int_0^1 (1-x^2)^{1/2} x \ln(1+\sqrt{1-x^2})\,dx \tag{20}$$

and

$$\epsilon_2 = a(\rho^2 - a^2)^{-1/2} - \sin^{-1}\frac{a}{\rho}. \tag{21}$$

In terms of (9) and (17), the total contact force in (3) can be written as:

$$P = -\frac{16H^3}{3CR}k_p;\ k_p = \frac{a^3}{\Delta H^3}. \tag{22}$$

The non-dimensional function k_p is calculated using an IBM 360/65 electronic computer, and its value is shown in Fig. 1.

As mentioned in the introduction, the critical point in the plate is at the surface point opposite the center of the contact area. The critical circumferential stress at this point can be determined for small value of H from eqn (33) in [7] for $r < a$ as follows:

$$\sigma_{\theta\theta}(r,-H) = -\frac{3}{4H^2}\int_0^a p(\lambda)\lambda \int_\lambda^\rho \int_0^\infty \left[\nu J_1(sm)J_0(sr) + (1-\nu)\frac{J_1(sr)J_1(sm)}{sr}\right] ds\,dm\,d\lambda. \tag{23}$$

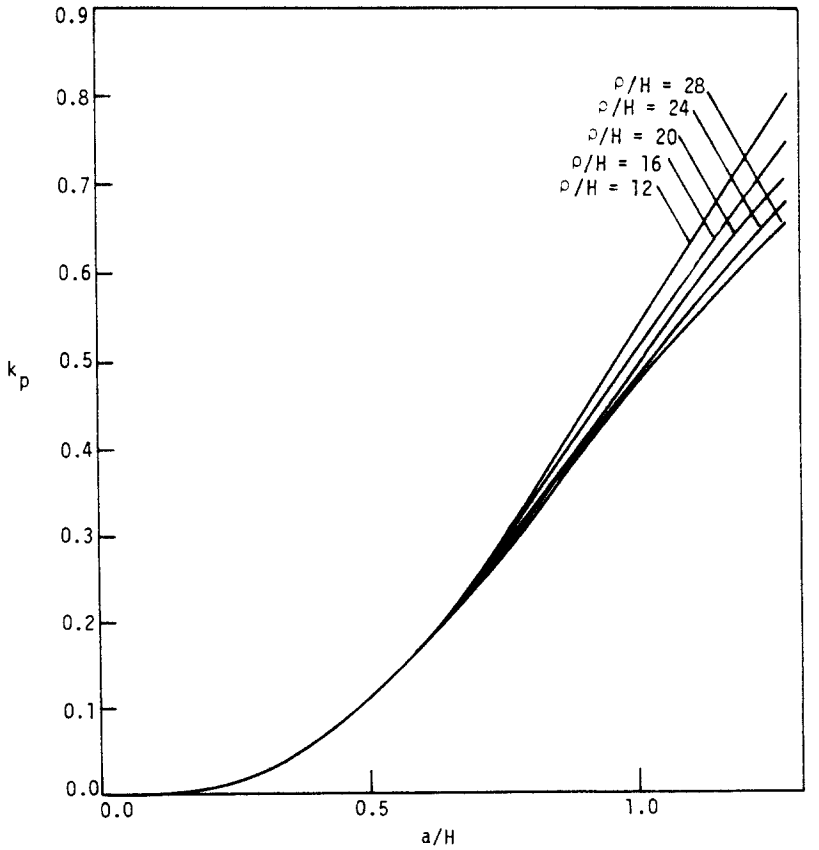

Fig. 1. Non-dimensional function k_p.

In integrating the above equation, the term A_1B_1 in eqn (6) is dropped, because it is of the order of a^3/ρ^3. The integrations in terms of (6) give the results[9] for $r < a$ as follows:

$$\frac{C\pi R\Delta H^2}{6}\sigma_{\theta\theta}(r,-H) = (1+\nu)\left\{\frac{1}{3}\ln\frac{\rho}{r}\left[a^3-(a^2-r^2)^{3/2}\right]+\right.$$
$$\left.\frac{1}{3}(a^2-r^2)^{3/2}\ln\rho-\int_r^a(a^2-\lambda^2)^{1/2}\lambda\ln\lambda\,d\lambda\right\}-$$
$$\frac{1-\nu}{6}\left\{\frac{2}{5}[a^5-(a^2-r^2)^{5/2}]\frac{1}{r^2}-a^3\right\}. \tag{24}$$

The critical stress can now be obtained from (24) for $r = 0$ as follows:

$$\sigma_{\theta\theta}(0,-H) = \frac{3P(1+\nu)}{8\pi H^2}\left(\ln\frac{\rho}{a}+D\right) \tag{25}$$

where the constant is

$$D = -3\int_0^1(1-x^2)^{1/2}x\ln x\,dx = 0.6399405. \tag{26}$$

FLEXURE STRENGTH

The flexure strength of a PMMA plate was studied experimentally for transverse quasi-static and impact loadings. For the quasi-static loading, the circular plate specimen with 10.16 cm (4 in.) diameter and 1.59 mm (1/16 in.) thickness was loaded by an 810 MTS machine with a ring foundation arrangement similar to that shown in [7]. The plate specimen was placed on the upper end of a tubular support made of hard steel. The cross section of the end was machined to be a smooth circular surface whose highest point forms a flat, smooth circle of 2.54 cm (1 in.) diameter. The other end of the tube was rigidly connected to a large flat steel plate, which was placed on the platform of the MTS machine. A steel ball of 4.445 cm ($1\frac{3}{4}$ in.) diameter was pressed by the machine onto the upper surface of the specimen. The ball was held by an adapter which was mounted to the machine cross-head. The system was aligned so that the center of the contact area between the specimen and the spherical indenter coincided with the center of the ring foundation. The specimen was loaded until fracture occurred. The rate of the vertical displacement of the machine was 0.254 mm/sec and the load required to fracture the specimen was measured as 189 N. A branching Y-shaped crack was observed as shown in Fig. 2.

The dynamic flexure strength of the PMMA plate specimen was experimentally investigated, using an impact system whose block diagram is shown in Fig. 3. The piezoelectric accelerometer employed was manufactured by Columbia Research Laboratories (Model 902). The system used here to record the signal output of the accelerometer is similar to that used in [11]

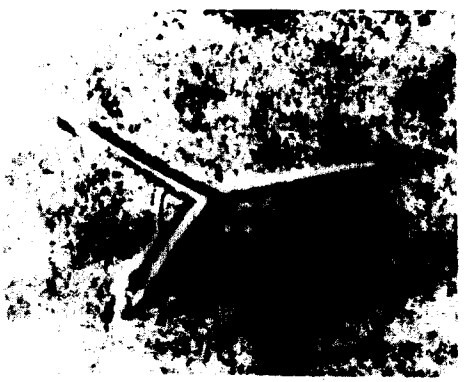

Fig. 2. Y-shaped flexure crack.

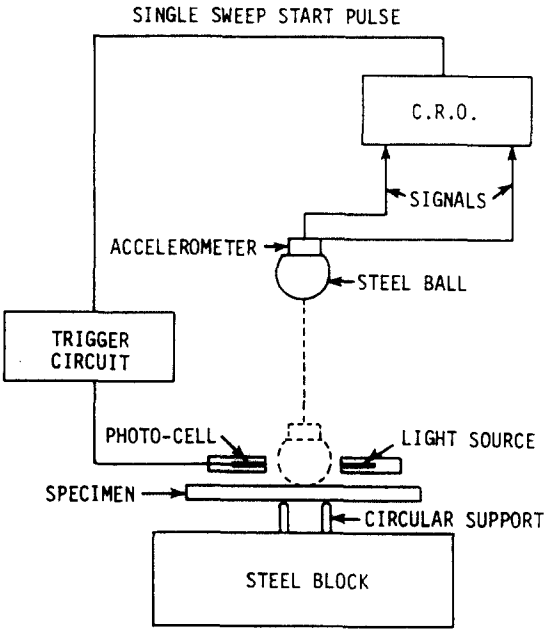

Fig. 3. Block diagram for the system of photographing accelerometer signal output.

for observing strain waves detected by strain gages. A circular ring support of 1 in. diameter, similar to that described above, was mounted on a vertical side of a $22.86 \times 22.86 \times 17.78$ cm steel block. A surface of the plate specimen was placed against the vertical end of the support, using light spring compressions. A 4.445 cm diameter steel ball was made to impinge onto the other surface of the specimen by releasing it from an electromagnet of a two-legged pendulum arrangement. The center of the contact area was aligned to coincide with the center of the support. A portion of the impacting steel ball, which was equal to the weight of the accelerometer, was cut off and the accelerometer was mounted on the flat cut-off side of the steel ball. The axis of the accelerometer was in the direction of impact which is normal to the specimen surface. The signal output of the accelerometer was fed to a cathode ray oscilloscope which has a wide band amplifier. In order to record the pulse shapes of the accelerometer output, the oscilloscope trace was triggered by arranging for the ball to traverse a thin beam of light, just before impinging on the plate specimen. The light beam was directed onto a small photocell so that an electrical impulse was produced, which when amplified could trigger the oscilloscope trace. The distance between the light and the specimen surface could be adjusted to produce the desired triggering delay time.

The outputs of the accelerometer were photographed from the screen of the oscilloscope and were shown in Fig. 4(a) and (b) for the same impact velocity of 110.21 cm/sec. This impact velocity was determined to be the value where the probability of occurrence of fracture was 50% [11, 12]. The smooth curve in Fig. 4(a) was the output for the case where fracture did not occur. The occurrence of fracture resulted in a sudden drop of the amplitude of the accelerometer output, as can be seen in Fig. 4(b). After the sudden drop in amplitude, the value of the curve recovered and increased to a new peak value. In other words, the plate specimen did not fail catastrophically and had a ballistic damage residual strength. This is similar to the ballistic impact response described in [13]. The shape of the crack produced by the dynamic load was observed to be similar to the Y-shaped crack shown in Fig. 2.

The value of the curve in Fig. 4(a) can be converted, in terms of the sensitivity of the accelerometer, into the acceleration of the impacting indenter, which can then be multiplied by the mass of the steel ball to obtain the force acting on the plate during the impact. The peak value in Fig. 4(a) was converted and gave the dynamic fracture load of 244.64 N, which is about 30% higher than the quasi-static fracture load presented above.

The critical stresses produced by the fracture loads in the plate specimen can be determined in terms of the material properties of the plate using the theory described above. PMMA is a

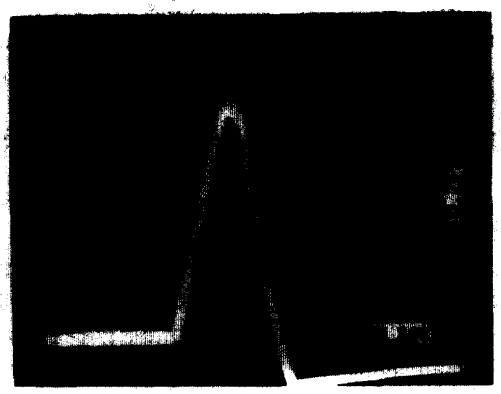

(a)

(b)

Fig. 4. Accelerometer output of an impacting indenter (a) no fracture (b) fracture occurring.

viscoelastic material whose properties depend upon the time rate of loading[14, 15]. For the impact test, the duration of loading is about 4 m sec, as can be seen in Fig. 4(a). Therefore Young's modulus is estimated as 5 GN/m^2 at 1.2×10^2 Hz and Poisson's ratio is estimated as 0.33[1]. The radius of the indenter R is 2.22 cm; the radius of the support span ρ is 1.27 cm ($\frac{1}{2}$ in.); and the plate thickness $2H$ is 1.59 mm. For the impact fracture load of 244.64 N, the value of k_p is calculated from eqn (22) in terms of the above data. For this value of k_p, the value of a/H is determined from Fig. 1 as 1.258. This, in turn, gives the radius of the contact area as 0.998 mm. From eqn (25) the critical stress at the lower surface point opposite the center of the contact area is determined as 196.23 MN/m^2. Similarly, for the quasi-static fracture load of 189 N, Young's modulus is estimated as 4 GN/m^2 and Poisson's ratio is estimated as 0.33[15]. The critical fracture stress is also calculated from eqn (25) as 152.86 MN/m^2. Therefore, the dynamic fracture stress is 28% higher than the quasi-static fracture stress. The finding that the critical stress is higher for dynamic loading than for static loading is consistent with that in [12].

CRACK PROPAGATION

The stress components in a plate can be written as the sum of the symmetrical (stretching) and antisymmetrical (bending) components when the plate is subjected to a flexure loading where it carries a transverse load on its upper surface and is supported by a foundation on its lower surface[7, 8]. For a crack produced in a glass plate specimen under a flexure loading, it was shown that the variation of the crack speed depends upon the in-plane average stretching stress. The magnitude of the stretching stress of the three-diemnsional stress field produced in the glass plate specimen was determined to be small, so that low flexure crack speed was produced and measured experimentally[8]. A study on PMMA plates similar to that for glass plates in [8] was carried out and presented in this section. Experimental arrangements for measuring crack speeds which are similar to those used in [8] were used, so that comparison can be made to the earlier work and flexure crack propagated far enough in PMMA plates for experimental measurements. The dimensions of the PMMA plate used for crack speed

measurements were $17.78 \times 7.62 \times 0.3175$ cm. The specimen was laid on the top of the ring foundation described above or on a knife-edge foundation which has two parallel supporting triangular edges with ridge radius of 0.4 mm, machined from a steel plate hardened through heat treatment[8]. The edges were all 6.35 mm long, but were made with different spans of $2L$. A steel ball of $1\frac{3}{4}$ in. diameter was mounted through an adapter to a hydraulic press. The ball was pressed onto the upper surface of the plate specimen. The center of the contact area between the indenter and the specimen was aligned to coincide with the center of the foundation in use, which was placed on the platform of the hydraulic press. In order to control the direction of fracture, a scratch was introduced starting at about 5 cm from the edge along the center line in the direction of the length on the lower plate surface. In front of the scratch, 10 silver lines of 6.35 mm apart were deposited, using a vacuum evaporator to form a grid as part of an electrical circuitry[8]. The silver lines were perpendicular to the direction of the scratch which is the expected direction of fracture. The load was applied until fracture occurred. When the crack was propagated, the passage of the crack broke the lines and generated voltage signals. The signals were fed to a cathode ray oscilloscope, and the trace on its screen was photographed giving the time required for the crack to propagate from one line to another. The photographs obtained are shown in Fig. 5 for different spans and supports. From the photographs and the spacing of the grid, the speed of the cracks was determined as a function of distance from the crack center as shown in Fig. 6.

The crack speeds in Fig. 6 varied from 1.3 m/sec to 13 m/sec and were small compared to the crack speeds of the previous glass specimens[8], which ranged from 36 m/sec to 476 m/sec. Since the in-plane stretching stress in the PMMA specimen was small[8], the crack speeds measured were also small compared to its limiting crack speed of 670 m/sec[16], as was the case for the glass specimens. The surface energy of PMMA is known to be about 1000 times as high as that of glass. This high value of the surface energy would cause a relatively large resistance to the propagation of a crack in PMMA. As a result, it can be seen in Fig. 6 that the crack speeds in the PMMA plates increased slowly in the initial stages and then oscillated until the specimens were completely fractured.

Fig. 5. Oscilloscope trace measuring the flexure crack speed (a) $2L = 2.54$ cm; (b) $2L = 0.635$ cm; (c) $2\rho = 2.54$ cm; (d) $2\rho = 0.635$ cm.

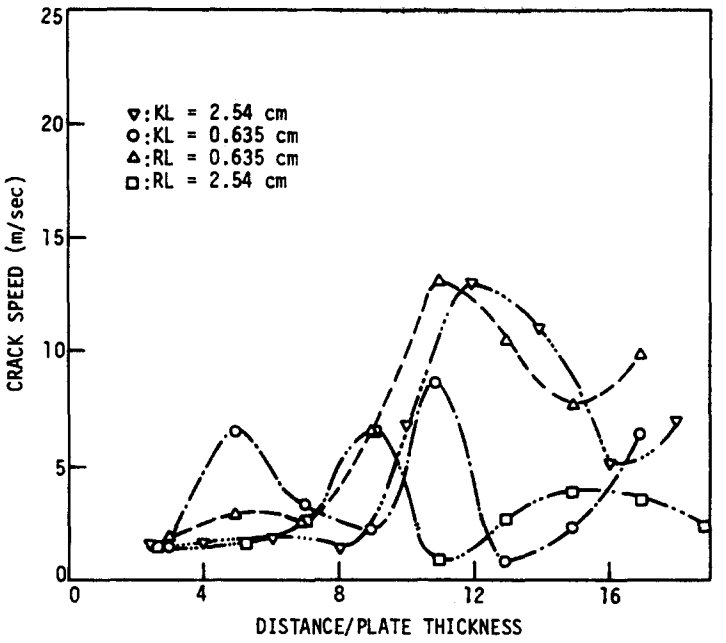

Fig. 6. Flexure crack speed measured experimentally at various distances from the loading point.

DISCUSSION AND CONCLUSIONS

The flexure strength and fracture of a PMMA plate resting on a ring foundation was investigated for transverse quasi-static and impact loadings. The quasi-static load was produced by pressing a steel ball onto the upper surface of the plate specimen using a MTS machine. The load required to produce fracture in the specimen was measured and Y-shaped fracture was observed as shown in Fig. 2. A piezoelectric accelerometer was used to measure the impact load which was produced by impinging a spherical steel indenter onto the surface of the PMMA plate specimen. The accelerometer system clearly detected the occurrence of fracture in the plate as a sudden drop in the amplitude of its output, as shown in Fig. 4(b). It can also be seen from the same figure that the failure of the plate is not catastrophic and that the plate has a ballistic damage residual strength[13].

The dynamic fracture load was measured, using the accelerometer, to be about 30% higher than the quasi-static fracture load. The pattern of the fracture produced by the impact load was observed to be similar to that shown in Fig. 2. The flexure fractures started at the critical point, which is at the surface of the plate opposite the center of the contact area between the indenter and the plate. The critical tensile stress at this point for the dynamic fracture load was determined to be 28% higher than the critical stress for the quasi-static fracture load.

The problem considered was treated as a problem of contact between a spherical body and a thin plate which was supported by a ring foundation. General eqns (6), (22) and (25) were obtained to determine, respectively, the normal contact stress, the radius of the contact area, and the critical tensile stress in the plate.

The speed of a crack propagating in a PMMA plate specimen was measured experimentally. The plate specimen was loaded on its upper surface and supported by a ring foundation or a knife-edge foundation[8]. Using the techniques of an electrically conductive grid, the crack speeds were measured to be ranging from 1.3 m/sec to 13 m/sec (Fig. 6). Since the in-plane stretching stress in the specimens was small[8], the crack speeds measured were small compared to the limiting crack speed of 670 m/sec[16].

Acknowledgement—This research was supported by the Engineering Research Institute, Iowa State University, Ames, Iowa 50011.

REFERENCES

1. L. C. Cessna, J. P. Lehane, R. H. Ralston and T. Prindle, The development of an instrumented projectile impact test: data on glass-reinforced and impact-modified polypropylene. *Polym. Engng Sci.* **16** (6), 419–425 (1976).
2. J. L. Preston, Jr. and T. S. Cook, Impact response of graphite-epoxy flat laminates using projectiles that simulate aircraft engine encounters. In *Foreign Object Impact Damage to Composites*, STP 568, ASTM, pp. 49–71 (1975).
3. L. B. Greszczuk and H. Chao, Impact damage in graphite-fiber reinforced composites. In *Composite Materials: Testing and Design*, STP 617, ASTM, pp. 389–408 (1977).
4. K. Marquerre and H. T. Woernle, *Elastic Plates*, p. 128. Blaisdell, Waltham, Mass. (1969).
5. L. H. Donnel, *Beams, Plates and Shells*, p. 224. McGraw-Hill, New York (1976).
6. R. J. Roark, *Formulas for Stress and Strain*, 4th edn, p. 216. McGraw-Hill, New York (1965).
7. Y. M. Tsai, Stress distribution and fracture produced by a spherical indenter in a glass plate resting on a ring foundation, *Dev. Mech.*, Vol. 5, (*Proc. 11th Midwestern Mech. Conf.* Edited by H. J. Weiss, *et al.*) 795–809 (1969).
8. Y. M. Tsai and Y. T. Chen, Propagation of a flexure crack: Experiment and analysis. *Int. J. Fract.* **14**, 281–291 (1978).
9. G. N. Watson, *Theory of Bessel Functions*, 2nd edn, p. 405. Cambridge University Press (1966).
10. S. G. Mikhlin, *Integral Equations*, p. 19. MacMillan, New York (1964).
11. Y. M. Tsai and H. Kolsky, A study of the fractures produced in glass blocks by impact. *J. Mech. Phys. Solids* **15**, 263–278 (1967).
12. Y. M. Tsai and H. Kolsky, A theoretical and experimental investigation of the flaw distribution on glass surfaces. *J. Mech. Phys. Solids* **15**, 29–46 (1967).
13. J. G. Avery and T. R. Porter, Comparisons of the ballistic impact response of metals and composites for military aircraft applications. In *Foreign Object Impact Damage to Composites*, STP 568, ASTM, pp. 3–29 (1975).
14. Y. M. Tsai and H. Kolsky, Surface wave propagation for linear viscoelastic solids. *J. Mech. Phys. Solids* **16**, 99–109 (1968).
15. B. E. Read and G. D. Dean, *The Determination of Dynamic Properties of Polymers and Composites*, p. 181. Adam Hilger (1978).
16. K. Katsamanis, D. Raftopuloe and P. S. Theocaris, The dependence of crack velocity on the critical stress in fracture. *Exp. Mech.* **17**, 128–132 (1977).